Neurochemical Research (2021) 46:183–196
https://doi.org/10.1007/s11064-020-03154-4

ORIGINAL PAPER

Short-Term Alterations in Behavior and Astroglial Function After Intracerebroventricular Infusion of Methylglyoxal in Rats

Lílian Juliana Lissner[1] · Leticia Rodrigues[1] · Krista Minéia Wartchow[1] · Ederson Borba[1] · Larissa Daniele Bobermin[1] · Fernanda Urruth Fontella[1] · Fernanda Hansen[2] · André Quincozes-Santos[1] · Diogo Onofre Gomes Souza[1] · Carlos-Alberto Gonçalves[1]

Received: 12 July 2020 / Revised: 12 October 2020 / Accepted: 15 October 2020 / Published online: 23 October 2020

Abstract

Methylglyoxal (MG) is a by-product of glycolysis. In pathological conditions, particularly diabetes mellitus, this molecule is unbalanced, causing widespread protein glycation. In addition to protein glycation, other effects resulting from high levels of MG in the central nervous system may involve the direct modulation of GABAergic and glutamatergic neurotransmission, with evidence suggesting that the effects of MG may be related to behavioral changes and glial dysfunction. In order to evaluate the direct influence of MG on behavioral and biochemical parameters, we used a high intracerebroventricular final concentration (3 μM/μL) to assess acute effects on memory and locomotor behavior in rats, as well as the underlying alterations in glutamatergic and astroglial parameters. MG induced, 12 h after injection, a decrease in locomotor activity in the Open field and anxiolytic effects in rats submitted to elevated plus-maze. Subsequently, 36 h after surgery, MG injection also induced cognitive impairment in both short and long-term memory, as evaluated by novel object recognition task, and in short-term spatial memory, as evaluated by the Y-maze test. In addition, hippocampal glutamate uptake decreased and glutamine synthetase activity and glutathione levels diminished during seventy-two hours after infusion of MG. Interestingly, the astrocytic protein, S100B, was increased in the cerebrospinal fluid, accompanied by decreased hippocampal S100B mRNA expression, without any change in protein content. Taken together, these results may improve our understanding of how this product of glucose metabolism can induce the brain dysfunction observed in diabetic patients, as well as in other neurodegenerative conditions, and further defines the role of astrocytes in disease and therapeutics.

Keywords Methylglyoxal · Cognitive dysfunction · Anxiety-like behavior · Glutamatergic metabolism · S100B

Introduction

Glycation has been associated with diabetes mellitus (DM), Alzheimer's disease (AD) and other chronic diseases [1–4]. α-Dicarbonyl compounds (α-DCs) (methylglyoxal [MG], glyoxal and 3-deoxyglucosone) are the principal molecules that cause protein glycation, due to their extremely reactive arrangement that can promote the fast formation of adducts [5]. In general, high concentrations of α-DCs lead to the increased formation of advanced glycation end products (AGEs) [5]. MG is a byproduct of glycolysis, and associations of the peripheral concentration of this physiological compound with pathophysiologic processes have been extensively studied [5, 6]. Despite the existence of different detoxification systems for excess MG, such as the glyoxalase system [7] impairments caused by increased concentrations of MG and other α-DCs are almost inevitable in some diseases.

Elevated MG levels are commonly associated with various DM complications, including chronic renal disease [3, 8], a faster rate of memory decline [4] and anxiety-like behavior [9]. Moreover, it is known that MG can affect neurotransmission, altering glutamatergic [10, 11] and GABAergic synapses [9]. Nonetheless, there have been few studies of the effects of MG on behavior and its association with neuroglial functions [10, 12].

✉ Carlos-Alberto Gonçalves
casg@ufrgs.br

[1] Federal University of Rio Grande do Sul (UFRGS), Biochemistry Post-Graduate Program, Ramiro Barcelos, 2600-Anexo, Porto Alegre, RS 90035003, Brazil

[2] Federal University of Santa Catarina (UFSC), Department of Nutrition, Nutrition Post-Graduate Program, Florianópolis, Brazil

Evidence suggests that the concentration of MG, in both the plasma and in cells, ranges from about 0.1–3 µM [5, 8]; however, these concentrations are 2–6 times higher in patients with DM [13]. Moreover, AD patients present an average MG concentration in the CSF of around 22 µM, which is far more significant than concentrations found in patients without AD [14]. Indeed, supraphysiological concentrations of MG have been used to study MG-related effects in *in vitro* and *in vivo* approaches [9–11, 15]. The challenge of mimicking the effects of MG using physiological or pathological concentrations is complex, especially considering MG reactivity and its rapid degradation in the organism. In order to simulate acute dicarbonyl stress, the use of high concentrations may aid in elucidating the mechanism of action of MG and its consequences, in experimental models.

Although there have been many efforts to elucidate the involvement of MG in DM complications and neurodegenerative diseases [14, 16], little is known about the *in vivo* acute effect on animal behavior and neuroglial functions. Studies have shown that repeated intracerebroventricular (ICV) administration of elevated concentrations of MG modulates anxiety-related behavior and neurochemical parameters in the rat brain [10, 15]. Herein, our focus was to investigate how an elevated MG concentration, directly infused in the lateral ventricle of rats, could acutely interfere with learning-memory processes, anxiety-related behavior and locomotor activity, and determine how astroglial modulation could be involved.

Experimental Procedure

Materials

Methylglyoxal (MG) solution (at 40%, in water), standard glutathione (GSH), Triton X-100, ophthaldialdehyde, S100B protein, anti-S100B (SH-B1), L-glutamate, o-phenylenediamine (OPD), meta-phosphoric acid, γ-glutamylhydroxamate acid and N-methyl-D-glucamine were purchased from Sigma-Aldrich (Saint Louis, MO, USA). L-[2,3-^{3}H] glutamate was purchased from Amersham International (United Kingdom). Polyclonal anti-S100B and polyclonal anti-GFAP were purchased from DAKO (São Paulo, SP, Brazil), anti-rabbit peroxidase linked antibody (GE Healthcare, Little Chalfont, United Kingdom). Polyclonal anti-GLAST and anti GLT-1 (Abcam, Cambridge, MA, USA), and polyclonal anti-glyoxalase 1 (Santa Cruz Biotechnology Inc. Dallas, Texas, USA). Mouse monoclonal anti-β-actin antibody (C4 clone), and mouse monoclonal anti-GluN1 (R1JHL clone) (Millipore, Darmstadt, Germany). All other chemicals were purchased from local commercial suppliers.

Animals

A total of seventy male Wistar rats (90-days old) were obtained from our breeding colony (Department of Biochemistry, UFRGS, Porto Alegre, Brazil). The rats were maintained under controlled light and environmental conditions (12 h light/12 h dark cycle, at a constant temperature of 22 ± 1 °C) and had free access to commercial chow and water. All animal experiments were carried out in accordance with the National Institute of Health Guide for the Care and Use of Laboratory Animals (NIH Publications No. 80-23), and all procedures were previously approved by the local Animal Care Ethical Committee (CEUA-UFRGS; project number 33663). All efforts were made to minimize animal suffering and reduce the number of animals used.

Surgical Procedure

MG was unilaterally infused in the lateral ventricle, as described in previous studies [10, 17]. The rats were divided into three groups: Naive (animals not submitted to surgical procedure), SHAM-operated and MG-treated. Briefly, rats were anesthetized with ketamine/xylazine (75 and 10 mg/kg, respectively, i.p) and positioned in a stereotaxic apparatus. A midline sagittal incision was made in the scalp and burr holes were drilled in the skull on the right side over the lateral ventricle. The right ventricle was accessed using the following coordinates: 0.9 mm posterior to the bregma; 1.5 mm lateral to the sagittal suture; 3.6 mm beneath the surface of the brain. Animals received 5 µL of MG ICV unilaterally with a final concentration of 3 µM/µL diluted in Hank's balanced salt solution (HBSS, pH 7.2); The SHAM group received an equal volume of HBSS. After the surgical procedure, animals were kept warm until recovery from anesthesia. From twelve hours after the ICV injection, the rats were submitted to behavioral assessments. The tasks were performed as follows: open field (OF) test and novel object-recognition task (NOR), elevated plus-maze (EPM) and Y-maze test. The behavioral tests were performed with different groups of animals, as follows: NOR was performed with different groups to those of the animals of the EPM and Y-maze test (performed together). Biochemical parameters were evaluated approximately seventy-two hours after ICV surgery.

Behavioral Tests

All behavioral experiments were performed at the active cycle of the animal (starting at 7 pm) and conducted in a sound-attenuated room under low-intensity light (12lx). The experimenters remained outside the room during the tests.

To avoid the presence of olfactory cues, all the testing apparatuses were cleaned with a 70% ethanol solution and dried with a paper towel after each trial.

Exposure to the Open Field (OF)

Motor activity was evaluated in the OF test. The OF apparatus consists of a square arena (60 × 60 cm) with dark wood and floor. The test consists of exposing the animals to this large arena where the central area is more aversive for rodents than the peripheral area and it is usually considered as an index of anxiety [18]. The rats were released in the corner of the arena to freely explore. The automated activity-monitoring system (Any-maze; Stoelting, Wood Dale, IL, USA) was used to measure the distance traveled over the arena and habituation. The distance traveled, as an index of general activity was registered twelve hours after surgery [10] modified.

Novel Object Recognition (NOR)

The cognitive performance was evaluated in the OF by the NOR task. This task comprised three distinct phases; habituation, training and discrimination devised by Ennaceur and Delacour [19] and adapted by Wartchow et al. [20]. The rats were placed in the corner of the arena to perform the task. In the habituation phase, the rats were allowed to explore the OF for ten minutes. Twenty-four hours after the habituation phase, the animals returned to the training trial: the rat was placed in the apparatus that contained two identical sample objects (A+A). After the end of the training trial, the rats were removed from the OF and kept in the home cage. One hour and twenty-four hours after the training trial, the rats returned to the apparatus to test short-term (STM) or long-term (LTM) memory, respectively. In the test session, the rat was returned to the OF arena that contained two objects; one object was identical to the training session and the other object was novel (A+B). For LTM, the object 'B' was replaced by a third one "C" (A+C), and the 'A' object was maintained the same. The time spent by the rats exploring each object was monitored with a video system placed in an adjacent room. Exploration of an object was defined as sniffing or touching the object with the nose. The recognition index was calculated based on time exploring the novel object×100/time exploring both objects [21–23].

Elevated Plus-Maze Test (EPM)

The elevated plus-maze test was used for evaluating anxiety-associated behavior [24] and was performed at twelve hours after surgery. The apparatus consisted of two opposing open arms (without walls) and two opposing closed arms (arms measured 45 × 10 cm), elevated 80 cm above the floor. On the day of the experiment, the animals were acclimated to the apparatus during one hour before the test. The rats were then placed individually on the central platform facing an open arm and were allowed to explore the maze for five minutes. Arm entry is defined as entering an arm with all four paws. The parameters analyzed here were the number of entries into the closed arms, entries into the open arms and the total time spent in each arm. The parameters of anxiety-like behavior are represented as percentage and calculated as follows: open arm (time exploring the open arm × 100/time exploring open and closed arms) or closed arm (time exploring the closed arm × 100/time exploring open and closed arms) [25].

Y-Maze

Thirty-six hours after surgery, the spatial memory of animals was investigated using the Y-maze paradigm. The apparatus consisted of three arms (50 × 10 × 20 cm and 120° apart) made of black wood placed in a room with visual cues on the walls. Y-maze testing consisted of two trials separated by an interval of one hour. In the first trial, 1 (of 3) arm was closed. The rats were placed at the end of one arm with their heads oriented in the opposite direction to the center of the maze and allowed to visit the 2 open arms for 5 min. In the second trial (one hour later), rats were placed back into the start arm of the maze with free access to all three arms for 5 min. The number of entries and the time spent in each arm were recorded. The index performance was calculated as follows: time exploring the novel arm × 100/time exploring the two other arms of the maze, except the arm in which the rat was first placed [26, 27].

Biochemical Analyses

Obtaining CSF, Serum and Hippocampal Samples

Animals were anesthetized and then positioned in a stereotaxic holder for CSF collection of 100 µL (approximately) from the cisterna magna. The puncture was performed using an insulin syringe (27 gauge X 1/2″ length). Rats were then removed from the stereotaxic apparatus and placed in a flat place; whole blood was obtained through an intracardiac puncture using a 0.37-mm diameter needle and was collected into clot activator tubes, centrifuged (3000 rpm, 10 min, 4 °C) to separate serum. The hippocampi were dissected and transverse of 0.3 mm were obtained using a McElwain Tissue Chopper. The samples were frozen at −80 °C until posterior analysis [28].

Glutamate Uptake Assay

Glutamate uptake was performed as previously described [29, 30]. Slices were incubated at 37 °C in HBSS and the assay was started by the addition of 0.1 mM L-glutamate and 0.66 µCi/mL L-[2,3-^{3}H] glutamate. Incubation was stopped after 5 min by removing the medium and rinsing the slices twice with ice-cold HBSS. The slices were then lysed in a 0.5 M NaOH solution. Sodium-independent uptake was determined using N-methyl-D-glucamine instead of NaCl. Sodium-dependent glutamate uptake (specific uptake) was obtained by subtracting the nonspecific uptake from the total uptake. Radioactivity was measured in a scintillation counter. Results were calculated as nmol/mg protein/min and were expressed as percentages of the SHAM.

CSF Glutamate Measurements by High Performance Liquid Chromatography (HPLC)

Glutamate levels in CSF were measured by HPLC, as previously described [31]. CSF samples were filtered and cell-free supernatant aliquots were used to quantify glutamate levels. The analysis was performed using a reverse phase column (Supelcosil LC-18, 250 mm × 4.6 mm × 5 µm, Supelco) in a Shimadzu liquid chromatograph (50 µL loop valve injection, 40 µL injection volume) and fluorescent detection after pre-column derivatization with *o*-phthalaldehyde. The mobile phase flowed at a rate of 1.4 mL/min and column temperature were 25 °C. Buffer compositions were as follows: Buffer A: 0.04 mol/L $NaH_2PO_4 \times H_2O$ buffer pH 5.5, containing 80% of methanol; B: 0.01 mol/L $NaH_2PO_4 \times H_2O$ buffer pH 5.5, containing 20% of methanol. The gradient profile was modified according to the content of buffer B in the mobile phase: 100% at 0.10 min, 90% at 15 min, 48% at 10 min, 100% at 60 min. Absorbance was read in a Shimadzu fluorescence detector. Samples of 20 µL were used and concentration was calculated in µM and was expressed as percentages of the SHAM.

Glutamine Synthetase (GS) Activity Assay

Enzymatic activity of glutamine synthetase (GS) was determined using the procedures described previously [32] with modifications. Briefly, slices were homogenized in 50 mM imidazole. Homogenates were incubated with (mM): 50 imidazole, 50 hydroxylamine, 100 L-glutamine, 25 sodium arsenate dibasic heptahydrate, 0.2 ADP, 2 manganese chloride, pH 6.2 for 15 min at 37 °C. The reactions were terminated by the addition of 0.2 mL of 0.37 M $FeCl_3$, 200 mM trichloroacetic acid, and 670 mM HCl. After centrifugation, the absorbance of the supernatant was measured at 530 nm and compared to the absorbance generated by standard quantities of γ-glutamyl hydroxamate acid treated with ferric chloride reagent. GS activity was calculated as µmol/mg protein/h and was expressed as percentages of the SHAM.

Reduced Glutathione (GSH) Content Assay

GSH levels were measured as described [33]. Slices were homogenized in sodium phosphate buffer (0.1 M, pH8.0) containing 5 mM EDTA and protein was precipitated with 1.7% meta-phosphoric acid. Supernatant was assayed with o-phthaldialdehyde (1 mg/mL methanol) at room temperature for 15 min. Fluorescence was measured using excitation and emission wavelengths of 350 and 420 nm, respectively. A calibration curve was employed using standard GSH solutions at concentrations ranging from 0 to 500 µM. GSH concentrations were calculated as nmol/mg protein and were expressed as percentages of the SHAM.

Glyoxalase Activity (GLO1) Assay

Hippocampal slices were lysed and homogenized in phosphate buffered saline (PBS), pH 7.4. Subsequently, slices were centrifuged at 13,000 rpm for 15 min at 4 °C and the supernatant was used for enzymatic activity and protein content measurements. GLO1 activity was assayed according to [10]. A unit of GLO1 activity is defined as the amount of enzyme that catalyzes the formation of 1 µmol of S-(D)-lactoylglutathione per minute. Specific activity was calculated in milliunits per milligram of protein (mU/mg protein) and was expressed as percentages of the SHAM.

Quantification of GFAP and S100B

Hippocampal, CSF and serum S100B contents were measured by an enzyme-linked immunosorbent assay (ELISA) [34]. Fifty µL of sample (previously diluted when necessary) plus 50 µL of Tris buffer were incubated for 2 h on a microtiter plate previously coated overnight with monoclonal anti-S100B (SH-B1) antibody. Polyclonal anti-S100 and peroxidase-conjugated anti-rabbit antibodies were incubated at the same time for 60 min at 37 °C. A colorimetric reaction with o-phenylenediamine was measured at 492 nm. The standard S100B curve ranged from 0.002 to 1 ng/mL. ELISA for hippocampal GFAP was performed as previously described [35] by coating the microtiter plate with 100 µL samples overnight at 4 °C. Incubation with a rabbit polyclonal anti-GFAP for 2 h was followed by incubation with a secondary antibody conjugated with peroxidase for 1 h, at room temperature; the standard GFAP curve ranged from 0.1 to 10 ng/mL. Data were calculated as ng/mg protein and were expressed as percentages of SHAM.

Immunohistochemical Staining of GFAP

Immunohistochemical staining of GFAP was performed according to [17]. The rats were anesthetized using ketamine/xylazine and perfused through the left cardiac ventricle with 200 mL of saline solution, followed by 200 mL of 4% paraformaldehyde in 0.1 M phosphate buffer, pH 7.4. The brains were removed and left for post-fixation in the same fixative solution at 4 °C for 2 h. The material was then cryoprotected by immersing the brain in 15% and 30% sucrose in phosphate buffer at 4 °C. The brains were sectioned (40 µm) on a cryostat (Leitz) and incubated with polyclonal anti-GFAP from rabbit (diluted 1:1000 in PBS-0.4% triton X-100 and 2% BSA) for 48 h at 4 °C. Subsequently, tissue sections were incubated with secondary anti-rabbit IgG Alexa Fluor 586 (A11011) (diluted 1:1000 in PBS) for 1 h at room temperature. Images were detected with the Olympus confocal microscope and analyzed in a computer with digital camera and Fluoviewer 3.1 FV1000 software.

Western Blotting Analysis of Glutamate Transporters (GLAST and GLT-1), Glutamate Receptor GLUN1 and GLO1

Equal amounts (20 µg) of proteins from each sample were boiled in a sample buffer [0.0625 M Tris–HCl pH 6.8, 2% (w/v) SDS, 5% (w/v) β-mercaptoethanol, 10% (v/v) glycerol, 0.002% (w/v) bromophenol blue] and separated by SDS-PAGE on 12% sodium dodecyl sulfate-polyacrylamide gel and electro transferred onto nitrocellulose membranes. The membranes were blocked overnight at 4 °C with 2% chicken egg albumin in Tris-buffered saline with Tween 20 (TTBS) and then incubated for 3 h at 4 °C with an anti-GLT-1 antibody (diluted 1:5000 in TTBS and 1% bovine standard albumin – BSA), or overnight with anti-GLAST, anti-GLUN1 and anti-GLO1 antibodies (diluted 1:5000 in TTBS and 1% BSA). Next, the membranes were incubated for 1h at room temperature with horseradish peroxidase (HRP)-conjugated anti-mouse or anti-rabbit secondary antibodies (diluted 1:10,000). Chemiluminescent bands were detected by image analyzer (Image Quant LAS4000 from GE) and optical density was quantified using ImageJ software. The results were expressed as percentages of the SHAM group.

RNA Extraction and Quantitative RT-PCR for S100B and IL-1β

Total RNA was isolated from hippocampal slices using TRIzol Reagent (Invitrogen, Carlsbad, CA). The concentration and purity of the RNA were determined spectrophotometrically at a ratio of 260:280. Extracted RNA (1 µg) was submitted to complementary DNA (cDNA) synthesis using a High Capacity cDNA Reverse Transcription Kit (Applied Biosystems, Thermo Fisher Scientific) in a 20 µL reaction, according to the manufacturer's instructions. Messenger RNA (mRNA) encoding S100B (#Rn04219408_m1) and IL-1β (#Rn00580432_m1) was quantified using the TaqMan real-time RT-PCR system, using inventory primers and probes purchased from Applied Biosystems [36]. Target mRNA levels were normalized to β-actin (#Rn00667869_m1) levels. Results were analyzed employing the $2^{-\Delta\Delta Ct}$ method [37] and expressed relative to the levels of the SHAM group.

Protein Determination

Protein content was measured by adapted Lowry's method using bovine serum albumin as standard [38].

Statistical Analysis

Data are reported as means ± standard errors and analyzed statistically by Student's *t*-test or one-way ANOVA, followed by Tukey's test. The NOR task was analyzed by a one-sample t-test to determine whether the recognition index was different from a chance performance (50%). Differences were considered significant when $p \leq 0.05$. All analyses were performed using the Prism 6.0 (GraphPad).

Results

Behavioral Effects

The experimental schedule used for all tests performed here is shown in Fig. 1. Initially, the present study investigated the acute effects of ICV-MG on the performance of rats in the OF task. The distance travelled was measured on day one (1), twelve hours after surgery, and was found to be diminished by MG injection, when compared to the SHAM group (Fig. 2a) ($F_{(2, 24)} = 10.27$, $p = 0.001$). Subsequently, the effect of MG administration was evaluated on cognitive performance using the training and discrimination phase in the NOR task. In the training phase, all groups evaluated did not present object preference/laterality, as indicated by the symmetric exploration of both familiar objects (Fig. 2b). In the discrimination phase, the MG group showed a decreased recognition index in both periods analyzed: STM (Fig. 2C) ($t_{(10)} = 0.286$, $p = 0.78$) and LTM (Fig. 2d) ($t_{(10)} = 0.665$, $p = 0.52$). Also, our study investigated the effects of MG injection on short-term spatial memory. The rats were exposed to a Y-maze task, thirty-six hours after surgery, and the number of entries and time spent in the novel arm were analyzed. There was a significant reduction in the time spent in the novel arm after MG infusion, suggesting an impairment in

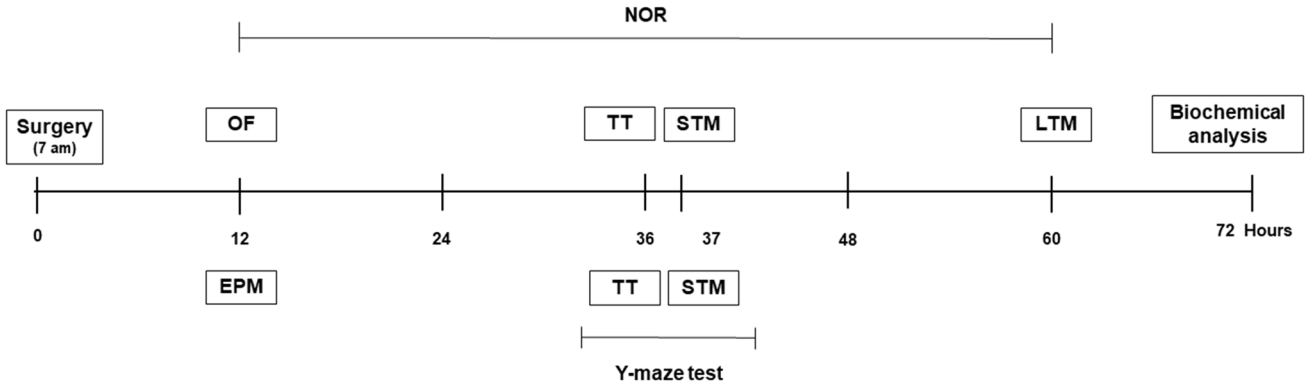

Fig. 1 Experimental timeline. Surgery corresponds to unilateral ICV infusion of MG (single injection of 5 µL with final concentration of 3 µM/µL or vehicle). Time is represented in hours after surgery. Behavioral tests were performed as follows: OF, NOR (training trial (TT), Short-time memory (STM) and Long-term memory (LTM)) of interval between each task, elevated plus maze (EPM) and Y-maze task. For biochemical analyses, cerebrospinal fluid, hippocampi and serum were harvested at seventy hours after the surgery

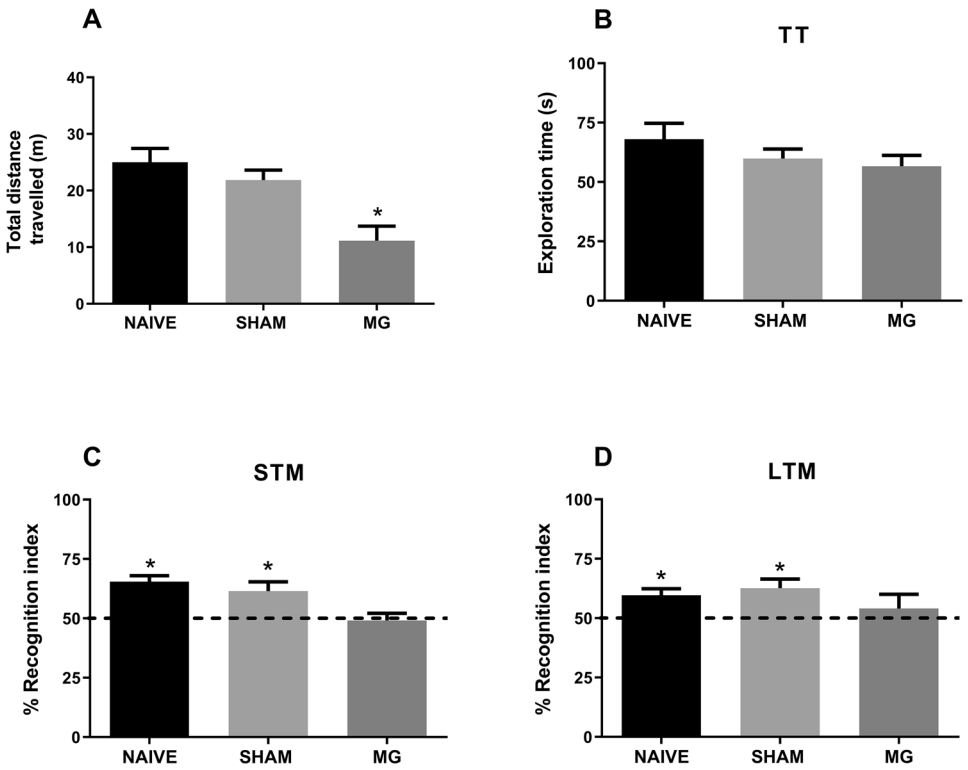

Fig. 2 Effect of ICV MG administration on locomotor activity and cognitive performance in the open field test. Locomotor activity was measured twelve hours after surgery (**a**) and cognitive performance was evaluated thirty-six hours by NOR test – TT (**b**), recognition index of STM (**c**) and LTM (**d**) after TT. Data are expressed as means ± SE (11–14 rats/group). The line in the graph indicates 50%. For graph A, * represents statistical difference from SHAM group (ANOVA followed by Tukey's test). For the other graphs, * represents statistical different group (one-sample *t*-test assuming $p < 0.05$, in which $p < 0.05$ versus chance level – 50% of novel object investigation in the discrimination phase)

spatial memory (Fig. 3a) ($F_{(2, 19)} = 6.11$, $p = 0.01$). Considering that MG is a $GABA_A$ agonist receptor, a reduction in anxiety-like behavior in rats in the EPM was expected. Data are presented in Table 1. Significant effects in the MG group were observed, as shown by the increase in time spent in the open arms ($F_{(2,17)} = 7.67$, $p = 0.0042$) and a decrease in entries in the closed arms ($F_{(2,20)} = 19.14$, $p < 0.0001$). These results indicate that MG presented an anxiolytic effect in this experimental design.

MG Infusion Decreased Glutamate Uptake in the Hippocampus

The glutamatergic system metabolism in hippocampal slices was investigated, approximately seventy-hours after ICV surgery. During neuronal activity, glutamate is released into the synaptic cleft and is rapidly taken up by excitatory amino acid transporters. Accordingly, the MG group presented a reduction of 25% in glutamate uptake (Fig. 4a, $p = 0.04$), when compared to SHAM. However, when we measured the

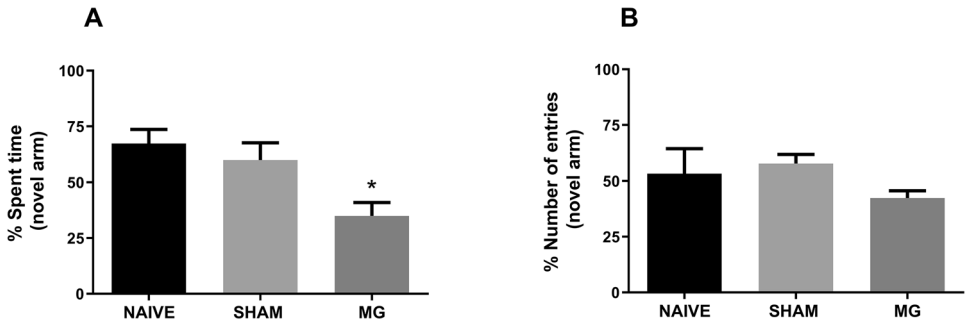

Fig. 3 Effect of ICV MG administration on spatial short-term memory, assessed in the Y-maze test. The percentage of total time spent in the novel arm (**a**) and the percentage of entries (**b**) in the novel arm during 5 min in the second trial are shown and were evaluated thirty-six hours after the ICV MG injection. Data are expressed as means ± SE (8 rats/group). *Represents statistical difference from SHAM group (ANOVA followed by Tukey's test, assuming $p < 0.05$)

Table 1 Effect of ICV MG administration on behavior in the elevated plus-maze test

Parameters			
	Naive	SHAM	Group MG
Time in open arms (s)	63.57 ± 18.60	67.78 ± 11.34	140.6 ± 40.68 *
Time in closed arms (s)	184.7 ± 11.48	158.9 ± 19.86	106.4 ± 42.26
Entries in open arms	5.714 ± 0.97	5.222 ± 0.85	4.429 ± 1.91
Entries in closed arms	11 ± 1.05	8.444 ± 1.25	1.571 ± 0.65 *
Percent time in open arms	29.36 ± 5.42	39.09 ± 8.56	79.45 ± 10.85 *
Percent time in closed arms	73.79 ± 5.55	58.99 ± 9.46	20.55 ± 10.85

Parameters were measured at twelve hours after surgery. Data are expressed as means ± SE (8 rats/group). *represents statistical difference from SHAM group (ANOVA followed by Tukey's test, assuming $p < 0.05$)

levels of glutamate in the CSF, no alterations were observed (Fig. 4b, $p = 0.80$). To determine whether the effect of MG on glutamate uptake was related to glutamate transporter levels, we compared the contents of GLAST and GLT-1 by Western blotting. However, no differences were observed in glutamate transporter immunocontent (Fig. 4c, $p = 0.19$; 4D, $p = 0.10$, respectively). Furthermore, the immunocontent of the GluN1 subunit of the NMDA glutamate receptor did not differ between groups (Fig. 4e, $p = 0.84$). With regard to GS activity, the enzyme that converts glutamate into glutamine, its hippocampal activity was diminished in response to MG ICV infusion (Fig. 4f, $p = 0.03$).

GSH Decreased by MG ICV Infusion

GSH content presented a decrease of approximately 60% following ICV infusion of MG, when compared to the SHAM group (Fig. 5a, $p < 0.0001$). Therefore, we investigated whether alterations in GLO1 activity or immunocontent could be involved in this effect, utilizing GSH as a cofactor, since GLO1 is a key enzyme in the glyoxalase system, participating in the detoxification of MG. No alterations in the activity of GLO1 or its immunocontent were observed following MG infusion, as indicated by Fig. 5b ($p = 0.43$) and Fig. 5c ($p = 0.88$), respectively.

Changes in Astroglial Markers After MG ICV Infusion

All the alterations in response to MG, observed so far (reduction in glutamate uptake and GSH content), are associated predominantly with astroglial functions. However, ELISA demonstrated that the levels of the major astroglial marker, GFAP, in the hippocampus were not significantly different in the MG group, when compared to the SHAM group (Fig. 6a, $p = 0.79$). Similar findings were demonstrated by immunohistochemistry for GFAP, which showed no apparent astrogliosis in CA1 during this short period of analysis (Fig. 6c). On the other hand, we observed an increase in the hippocampal expression of the pro-inflammatory cytokine, interleukin-1β (IL-1β) was increased in the MG group (Fig. 6b, $p = 0.02$), suggesting an acute inflammatory scenario in the hippocampus, without changes in GFAP. Concomitantly, it was observed a decrease in hippocampal S100B mRNA expression (another typical astroglial marker) in the MG group (Fig 7a, $p = 0.03$), with a significant increase in CSF S100B content in the MG group, compared to the SHAM group (Fig. 7c, $p = 0.01$). However, no changes in hippocampal S100B protein content (Fig. 7b, $p = 0.307$) or serum S100B levels (Fig. 7d, $p = 0.41$) were observed.

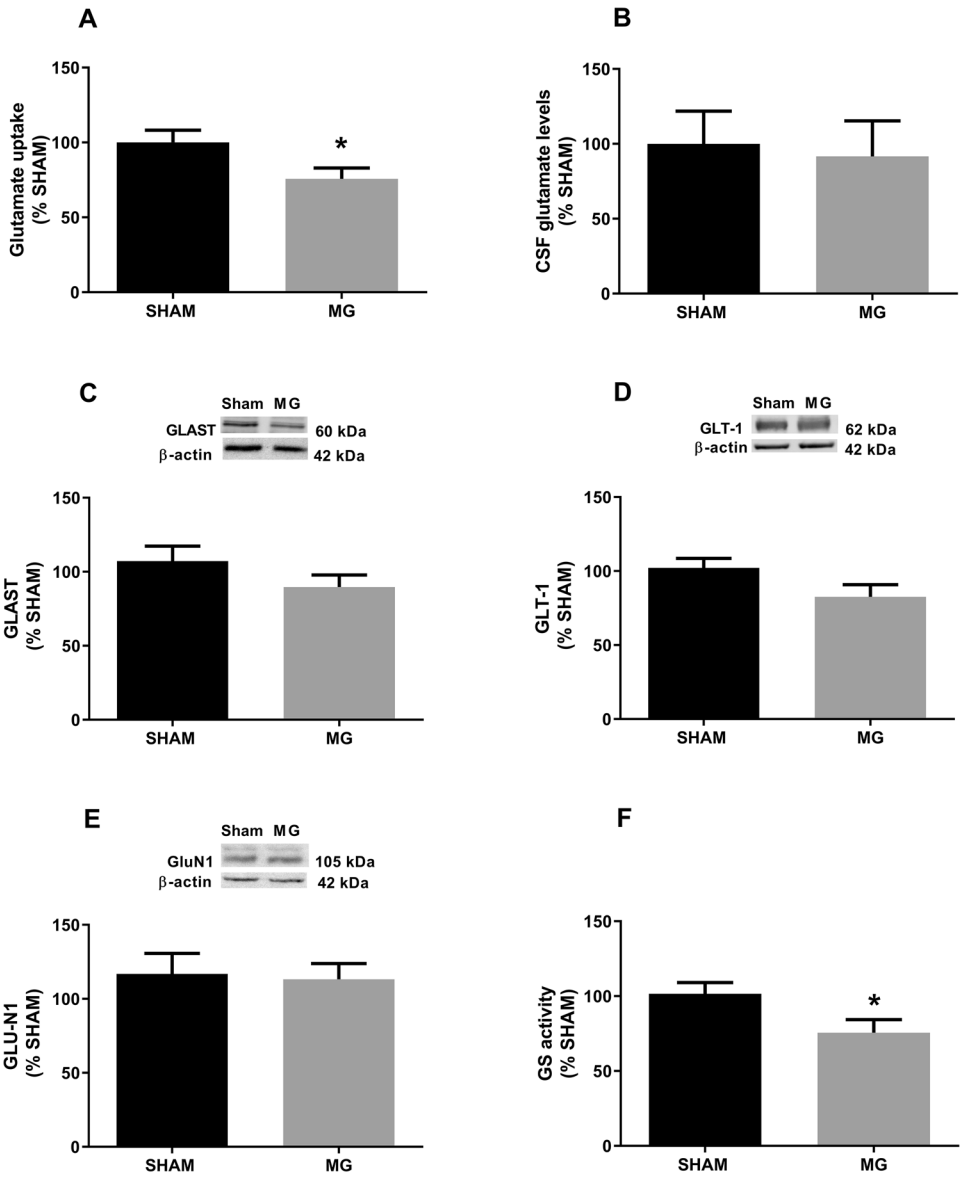

Fig. 4 Effect of ICV MG administration on the glutamatergic system in the hippocampus and cerebrospinal fluid. Glutamate uptake in hippocampal slices (N = 11) (**a**) and CSF levels of glutamate (N = 5) (**b**) were measured by HPLC seventy-two hours after surgery. Immunocontent of hippocampal glutamate transporters (GLAST and GLT1) (**c**, **d**) and NMDA receptor (GLUN1) (**e**), measured by Western blotting (N = 5 – 10) and GS activity (N = 13) (**f**). Data are expressed as means ± SE, assuming SHAM value as 100%. SHAM values of glutamate uptake and GS activity were 0.57 nmol/mg protein/min and 9.81 µmol/mg protein/h, in the hippocampus, respectively. *represents statistical difference from SHAM group (Student's *t*-test, assuming $p < 0.05$)

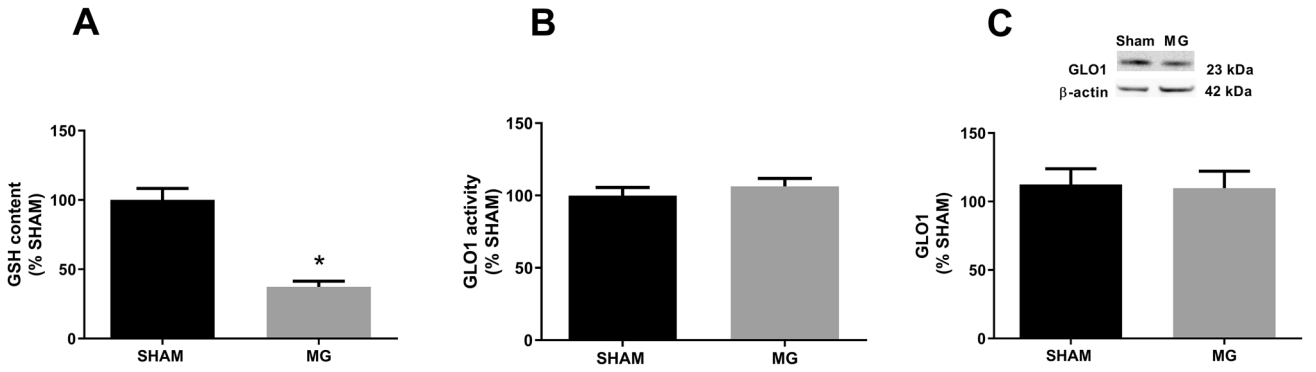

Fig. 5 Effect of ICV MG administration on GSH content, GLO1 activity and content in hippocampus. In (a), GSH content was measured by fluorometric method (N = 13), GLO1 activity by kinetic reaction (N = 13) (**b**) and GLO1 content was determined by Western blotting (N = 5) (**c**), at seventy-two hours after surgery. Data are expressed as means ± SE assuming SHAM value as 100%. SHAM values were: GSH, 19.16 nmol/mg protein; GLO1 activity, 215.15 mU/mg protein. *represents statistical difference from SHAM group (Student's *t*-test, assuming $p < 0.05$)

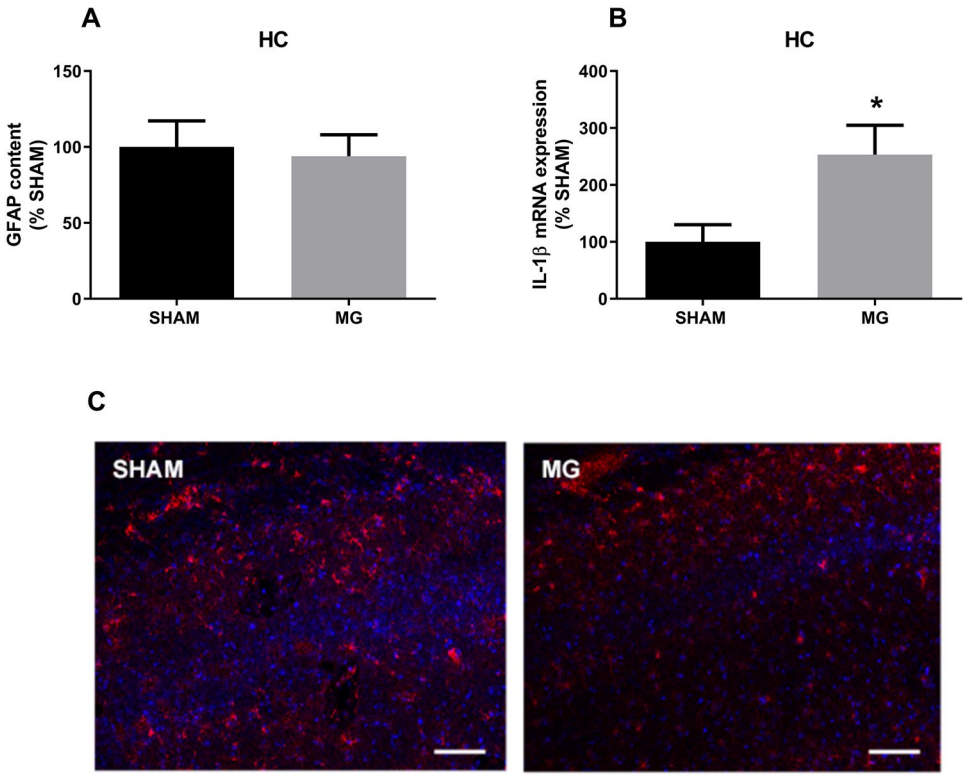

Fig. 6 Effect of ICV MG administration on GFAP content and IL-1β mRNA expression. Hippocampal slices of rats were dissected out at seventy-two hours after surgery and the following were determined; GFAP by ELISA (N = 13) (**a**), IL-1β mRNA expression (N = 8) (**b**) and immunohistochemistry for GFAP (**c**) magnified by 10X by confocal microscopy. Scale bars = 150 µm. Data are expressed as means ± SE, assuming SHAM value as 100%. SHAM values of GFAP: 35.25 nmol/mg. *represents statistical different from SHAM group (Student's *t*-test, assuming $p < 0.05$)

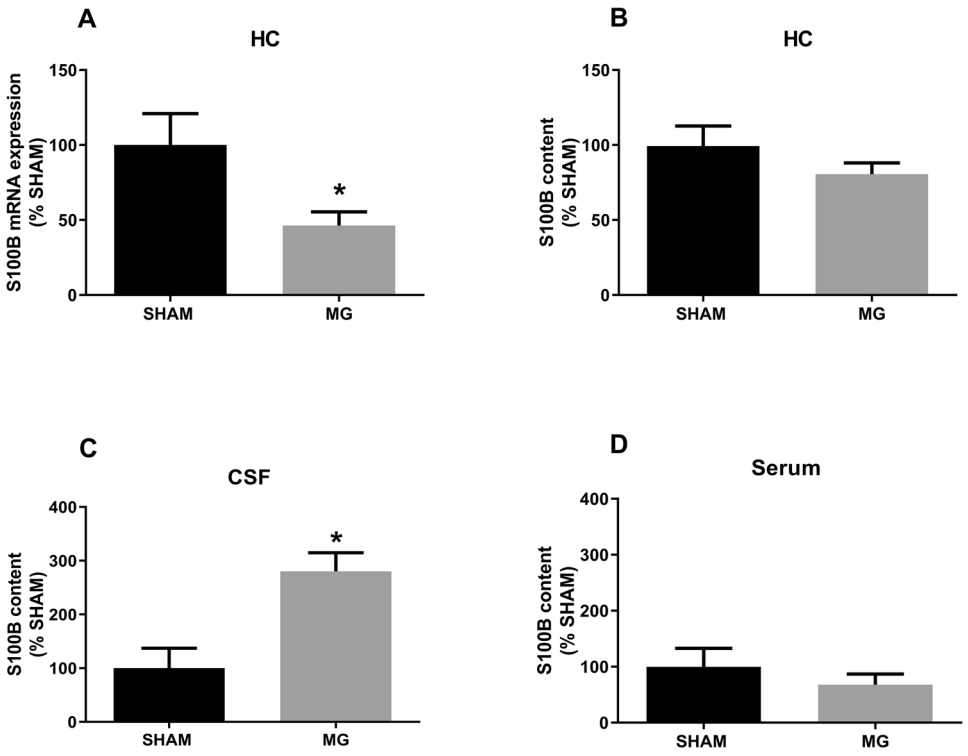

Fig. 7 Effect of ICV MG administration on the astroglial marker, S100B. Hippocampal slices of rats were dissected out at seventy-two hours after surgery and S100B mRNA expression (N = 8) (**a**) and S100B content (N = 13) (**b**) were evaluated. S100B levels in CSF (N = 5) (**c**) and serum (N = 8) (**d**) were also measured by ELISA. Data are expressed as means ± SE assuming SHAM as 100%. SHAM values of S100B content were 0.67 nmol/mg protein in the hippocampus, and 0.51 and 0.063 ng/mL protein in the CSF and serum, respectively. *represents statistical difference from SHAM group (Student's *t*-test, assuming $p < 0.05$)

Discussion

The dysfunction in glucose metabolism and generation of reactive intermediate metabolites as MG contribute to the metabolic complications observed in diabetic patients as well as to brain damage observed in neurodegenerative disorders, including Alzheimer's disease [39, 40]. In recent years, the relation between hyperglycemia in consequence of poor controlled diabetes and the development of cognitive deficiency as well as a greater propensity to the development of Alzheimer's disease has been extensively studied [41, 42]. Previous findings have shown that MG or MG-mediated glycation could be, at least in part, responsible for the faster cognitive decline presented in these disorders and also in older individuals [14, 43, 44]. Furthermore, MG can exacerbate cellular response, increasing oxidative stress and inflammation [45–48]. In the central nervous system, previous studies have suggested that astrocytes are more susceptible to damage of dicarbonyl stress caused by elevated levels of MG, once they are key players in neuroprotection and modulation of glutamatergic system [49].

The present study aimed to understand how an acute high concentration of methylglyoxal (administered by ICV infusion) modulates behavioral and neurochemical parameters in rats, with particular attention to astroglial function. Previous studies have shown that, at concentrations considered to be physiological (μM), MG acts as a partial agonist of $GABA_A$ receptors, and that acute elevated levels of MG induce locomotor depression and ataxia [9]. Accordingly, we found that a high concentration of MG (3 μM/μL) evoked a decrease in locomotor activity in the OF assessment, as seen by the reduction in the total distance travelled in the OF (twelve hours after surgery). Previous reports have also demonstrated similar effects on $GABA_A$ receptor activation [9, 15]. Concomitantly, our results indicated that acute MG infusion was able to generate anxiolytic-related behavior in rats (as evaluated by the plus maze task), as shown by the increase in time spent in the open arms. In addition to $GABA_A$ activation, MG levels can modulate GLO1 activity, the rate limiting step enzyme of the glyoxalase system [50]. In a chronic mouse model of inhibition of GLO1 expression, increased MG levels caused a decrease in anxiety-like behavior [51, 52]. MG has been also reported to show an acute anxiolytic effect [9, 12] and the daily injection of this molecule in rats reduced anxiety like-behavior [15]. Taken together, data suggest that anxiety behavior is dependent on the time of exposure and that acute MG administration affects this behavior.

For cognitive performance analysis, two different learning and memory tasks were performed. Firstly, in the NOR test, we found that MG-treated rats showed a decline in STM and LTM, consistent with the impairment in short-term spatial memory, evaluated by the Y-maze. Herein, we found that a cognitive deficit occurred in a brief period of time (thirty-seven hours after surgery) in different memory types. Our data corroborate those of previous studies, which suggest that MG induces a cognitive deficit within a short time [12]. Previous studies have demonstrated that MG accumulation, common in aged or diabetic patients, may be related to cognitive deficits [46]. A high serum level of MG was associated with a faster rate of cognitive decline [53, 54] and may contribute to the decline in executive function performance and memory in non-demented elderly patients [55]. In addition, reports have shown that MG cell treatment induces apoptosis in hippocampal neurons via an impairment of mitochondrial functions [45]. It should be noted that MG acts as a potent precursor for AGEs, which in turn are associated to cognitive dysfunction [56]. However, we did not investigate AGE/RAGE signaling, but considering the high dose and short protocol for administration, we suggest that both mechanisms - glycation and a direct effect on receptor - may be involved in the events observed.

The impairment of glutamate metabolism in astrocytes may be the basis of the cognitive deficit, induced by MG. In fact, MG decreased the glutamate uptake in hippocampal slices. This decrease was not accompanied by a decrease in the major astroglial glutamate transporters, GLAST and GLT-1, which is in agreement with other studies which indicated no differences in astrocyte glutamate transporter levels in an animal model of DM [57]. Aminoguanidine, an antiglycant compound, prevented the effect of MG on glutamate uptake in astrocyte cultures [11]. Therefore, the decrease in the activity of these transporters observed in hippocampal slices may be caused directly by glycation. Further investigating the glutamatergic system, we did not observe changes in the hippocampal content of GLUN1, a subunit of the NMDA glutamate receptor commonly involved in the glutamate excitotoxicity. This absence of alteration in GLUN1 does not exclude the possibility of excitotoxicity caused by a reduced astroglial glutamate uptake. However, a possible elevation of extracellular levels of glutamate was not confirmed by an increase in CSF glutamate. Such glutamate elevation in CSF would reinforce glutamate excitotoxicity, but its absence also does not exclude this possibility, since glutamate levels in the CSF do not reflect necessarily the extracellular levels of this neurotransmitter in the hippocampus.

Importantly, we observed a decrease in the activity of GS, the enzyme that converts glutamate to glutamine, which in turn is released to neuronal glutamate synthesis. GS in the brain tissue is exclusively glial and GS decrease impairs the glutamate-glutamine cycle and, consequently, glutamatergic

transmission [58, 59]. It seems clear that elevated MG affects astroglial function and that this, consequently, changes important systems of neurotransmission, which could also contribute to explain the memory impairment observed here.

The glyoxalase system, as discussed before, is responsible for preventing MG-induced dicarbonyl stress. This enzymatic pathway is dependent mainly on the endogenous antioxidant, GSH [50]. In our study, MG administration caused a depletion in GSH content, which was observed seventy hours after surgery. Nonetheless, GLO1 activity and protein expression were not significantly altered in the hippocampus. A previous study in astrocyte cultures demonstrated that GLO1 activity is increased at twenty-four hours after MG exposure [11]. We cannot rule out a fast and transient increment of GLO1 *in vivo*, but we only measured this enzyme seventy-hours after MG insult. GSH is an important antioxidant in the brain tissue, and is mainly produced and recycled by astrocytes [60]; as such, its decrease indicates astrocyte dysfunction; the decrease in GSH content observed may be explained, in part, by MG consumption, in turn forming S-D-lactoylglutathione, the substrate of GLO1. Thus, MG traps GSH. On the other hand, a decrease in GSH content may be explained by the decrease in glutamate uptake, since glutamate is a substrate for GSH synthesis [61]. Notably, GSH is exported by astrocytes to maintain GSH levels in neurons, via astrocyte-neuron shuttles for GSH. Moreover, extracellular GSH can also act as a neuromodulator of the glutamatergic system. In fact, at this point, it is necessary to consider that the action of MG (beyond protein glycation and the *per se* effect on GABA receptors) alters the concentration of two other neuroactive compounds. It causes an increase in D-lactate (the product of MG detoxification) and a decrease in GSH, which can affect glutamatergic, GABAergic and dopaminergic neurotransmission (see [6] for a review) and may also explain the cognitive deficit induced by MG here.

S100B is a calcium-binding protein that is predominantly expressed and secreted by astrocytes [62]. Extracellular S100B has been used as a marker of glial activation in response to injury stimuli [63]. Herein, we observed an increase in CSF S100B; however, the increase in CSF S100B was not accompanied by changes in serum S100B, confirming the idea that changes in CSF S100B are not necessarily related to serum S100B [64]. It is already known that CSF S100B is elevated in response to acute brain injury conditions [64, 65] and earlier stages of AD [66]. A decrease in hippocampal mRNA levels of S100B was also observed, without a corresponding decrease in S100B protein content. Changes in S100B mRNA do not necessarily accompany changes in the protein content [67], but note that we measured S100B parameters only at seventy-hours and, in further studies, other time points could allow us to better understand such variations. In addition to the increase in extracellular S100B, we observed an upregulation of the mRNA for interleukin-1β (IL-1β), suggesting an inflammatory process induced by MG, possibly by activation of RAGE. S100B both stimulates primary inflammatory cytokines (e.g. IL-1beta) and responds to them [68, 69]. Extracellular S100B functions as a neurotrophic cytokine and has, more recently, been considered an alarmin [70, 71].

In contrast, we did not find changes in GFAP hippocampal content (measured by ELISA), or in CA1 hippocampal region (evaluated by immunohistochemistry). Although there are only a few studies that show hippocampal GFAP alterations in MG-treated rats, this finding is in agreement with those of our previous study [10]. Conversely, MG administration has been shown to induce hippocampal astrocyte reactivity (GFAP and S100B increases), as reported by Chu et al. [72], however, this divergence could be explained by methodological differences, since authors evaluated astrocyte reactivity after chronic MG treatment (6 weeks after daily MG i.p doses). The cited study also reported an inflammatory response to MG, in which the c-Jun-N-terminal-kinase (JNK) pathway was strongly activated which may be related also to upregulation of IL-1β mRNA confirmed in this study.

Therefore, the ability of MG to affect astrocyte-neuron glutamatergic metabolism is quite clear. However, the precise mechanism by which this occurs deserves further investigation. MG-induced damage may be due to RAGE activation or to the direct glycation of cellular signaling pathways in brain tissue. This means that signaling pathways in neurons could be directly affected by MG or via RAGE [46]. In spite of this direct effect on neurons, our data indicate an important involvement of astrocytes in the brain injury induced by ICV administered MG. MG-induced brain damage was confirmed by cognitive deficit in behavioral tasks that depend on hippocampal functional integrity. In the hippocampal tissue, we found reduced glutamate uptake activity, as well as a decrease in GS activity and reduced levels of GSH. It is possible that MG directly, or via RAGE, caused astrocyte dysfunction, which in turn affected neuronal signaling and cognitive performance. Changes in glutamate uptake and GS activity, caused by elevated levels of MG, affected glutamatergic communication, and may alter the levels of other compounds that modulate synapses, such as D-lactate and GSH. Our data contribute to understanding MG toxicity and place astrocytes as targets and mediators of this toxicity.

It is important to mention some limitations of this study. Firstly, the MG concentration under pathological conditions (e.g. DM) is lower than that used in this study. However, this concentration was based on previous study that employed the administration of MG by ICV and seemed adequate for the investigation of the acute effect of this compound. Secondly, euthanasia was performed only seventy hours after the administration of MG. Shorter times would allow a better

correlation between neurochemical changes and behavioral changes. Finally, we used a commercial MG and did not analyze the purity of this compound. We cannot exclude the possibility that impurities may have contributed to the observed effects.

Conclusions

Acute ICV administration of MG impairs short- and long-term learning and memory processes, based on the NOR and Y-maze tasks, which depend on hippocampal functional integrity. In the hippocampal tissue, we found reduced glutamate uptake and GS activity, as well as reduced levels of GSH. In association with changes in S100B, these data suggest that astrocytes are targets of MG toxicity, despite displaying high activity of the glyoxalase system, which eliminates this metabolite. All these possibilities reinforce the role of astrocytes in neurotransmission and place them as targets of MG toxicity, suggesting their participation in neurodegenerative diseases such as DM and AD.

Acknowledgments The authors gratefully acknowledge the Conselho Nacional de Desenvolvimento Científico e Tecnológico (CNPq), Coordenação de Aperfeiçoamento de Pessoal de Nível Superior (CAPES), Fundação de Amparo à Pesquisa do Estado do Rio Grande do Sul (FAPERGS) and Instituto Nacional de Ciência e Tecnologia para Excitoxicidade e Neuroproteção (INCTEN/CNPq).

Contribution Statement F.H., C.A.G. and L.J.L. designed the study. L.J.L., E.B., L.R., K.M.W., L.D.B., F.U.F., F.H performed laboratory experiments and collected data. L.J.L. and K.M.W performed statistical analyses. F.H., C.A.G., L.J.L, K.M.W., L.D.B and L.R. wrote the manuscript. All authors edited and approved the manuscript.

Disclosure of Potential Conflicts of Interest The authors declare that they have no conflicts of interest.

Data Availability The data used to support the findings of this study are available from the corresponding author upon request.

References

1. Ahmed N, Ahmed U, Thornalley PJ et al (2005) Protein glycation, oxidation and nitration adduct residues and free adducts of cerebrospinal fluid in Alzheimer's disease and link to cognitive impairment. J Neurochem 92:255–263. https://doi.org/10.1111/j.1471-4159.2004.02864.x
2. Beisswenger PJ (2014) Methylglyoxal in diabetes: link to treatment, glycaemic control and biomarkers of complications. Biochem Soc Trans 42:450–456. https://doi.org/10.1042/BST20130275
3. Beisswenger PJ, Howell SK, Russell GB et al (2013) Early progression of diabetic nephropathy correlates with methylglyoxal-derived advanced glycation end products. Diabetes Care 36:3234–3239. https://doi.org/10.2337/dc12-2689
4. Cai W, Uribarri J, Zhu L et al (2014) Oral glycotoxins are a modifiable cause of dementia and the metabolic syndrome in mice and humans. Proc Natl Acad Sci USA 111:4940–4945. https://doi.org/10.1073/pnas.1316013111
5. Rabbani N, Thornalley PJ (2015) Dicarbonyl stress in cell and tissue dysfunction contributing to ageing and disease. Biochem Biophys Res Commun 458:221–226. https://doi.org/10.1016/j.bbrc.2015.01.140
6. Gonçalves C-A, Rodrigues L, Bobermin LD et al (2018) Glycolysis-derived compounds from astrocytes that modulate synaptic communication. Front Neurosci 12:1035. https://doi.org/10.3389/fnins.2018.01035
7. Ahmed N, Thornalley PJ (2003) Quantitative screening of protein biomarkers of early glycation, advanced glycation, oxidation and nitrosation in cellular and extracellular proteins by tandem mass spectrometry multiple reaction monitoring. Biochem Soc Trans 31:1417–1422. https://doi.org/10.1042/bst0311417
8. Wang X-J, Ma S-B, Liu Z-F et al (2019) Elevated levels of α-dicarbonyl compounds in the plasma of type II diabetics and their relevance with diabetic nephropathy. J Chromatogr B Analyt Technol Biomed Life Sci 1106–1107:19–25. https://doi.org/10.1016/j.jchromb.2018.12.027
9. Distler MG, Plant LD, Sokoloff G et al (2012) Glyoxalase 1 increases anxiety by reducing GABAA receptor agonist methylglyoxal. J Clin Invest 122:2306–2315. https://doi.org/10.1172/JCI61319
10. Hansen F, Pandolfo P, Galland F et al (2016) Methylglyoxal can mediate behavioral and neurochemical alterations in rat brain. Physiol Behav 164:93–101. https://doi.org/10.1016/j.physbeh.2016.05.046
11. Hansen F, Galland F, Lirio F et al (2017) Methylglyoxal induces changes in the glyoxalase system and impairs glutamate uptake activity in primary astrocytes. Oxidative Med Cell Longev 2017:9574201. https://doi.org/10.1155/2017/9574201
12. Szczepanik JC, de Almeida GRL, Cunha MP, Dafre AL (2020) Repeated methylglyoxal treatment depletes dopamine in the prefrontal cortex, and causes memory impairment and depressive-like behavior in mice. Neurochem Res 45:354–370. https://doi.org/10.1007/s11064-019-02921-2
13. Phillips SA, Thornalley PJ (1993) The formation of methylglyoxal from triose phosphates. Investigation using a specific assay for methylglyoxal. Eur J Biochem 212:101–105. https://doi.org/10.1111/j.1432-1033.1993.tb17638.x
14. Kuhla B, Lüth H-J, Haferburg D et al (2005) Methylglyoxal, glyoxal, and their detoxification in Alzheimer's disease. Ann N Y Acad Sci 1043:211–216. https://doi.org/10.1196/annals.1333.026
15. Hambsch B, Chen B-G, Brenndörfer J et al (2010) Methylglyoxal-mediated anxiolysis involves increased protein modification and elevated expression of glyoxalase 1 in the brain. J Neurochem 113:1240–1251. https://doi.org/10.1111/j.1471-4159.2010.06693.x
16. Allaman I, Bélanger M, Magistretti PJ (2015) Methylglyoxal, the dark side of glycolysis. Front Neurosci 9:23. https://doi.org/10.3389/fnins.2015.00023
17. Rodrigues L, Wartchow KM, Suardi LZ et al (2019) Streptozotocin causes acute responses on hippocampal S100B and BDNF proteins linked to glucose metabolism alterations. Neurochem Int 128:85–93. https://doi.org/10.1016/j.neuint.2019.04.013
18. Heredia L, Torrente M, Colomina MT, Domingo JL (2014) Assessing anxiety in C57BL/6J mice: a pharmacological characterization of the open-field and light/dark tests. J Pharmacol Toxicol Methods 69:108–114. https://doi.org/10.1016/j.vascn.2013.12.005
19. Ennaceur A, Delacour J (1988) A new one-trial test for neurobiological studies of memory in rats. 1: behavioral data. Behav Brain Res 31:47–59
20. Wartchow KM, Rodrigues L, Lissner LJ et al (2020) Insulin-producing cells from mesenchymal stromal cells: protection against

cognitive impairment in diabetic rats depends upon implant site. Life Sci 251:117587. https://doi.org/10.1016/j.lfs.2020.117587
21. Benice TS, Rizk A, Kohama S et al (2006) Sex-differences in age-related cognitive decline in C57BL/6J mice associated with increased brain microtubule-associated protein 2 and synaptophysin immunoreactivity. Neuroscience 137:413–423. https://doi.org/10.1016/j.neuroscience.2005.08.029
22. Borsoi M, Antonio CB, Viana AF et al (2015) Immobility behavior during the forced swim test correlates with BNDF levels in the frontal cortex, but not with cognitive impairments. Physiol Behav 140:79–88. https://doi.org/10.1016/j.physbeh.2014.12.024
23. Broadbent NJ, Gaskin S, Squire LR, Clark RE (2010) Object recognition memory and the rodent hippocampus. Learn Mem 17:5–11. https://doi.org/10.1101/lm.1650110
24. Walf AA, Frye CA (2007) The use of the elevated plus maze as an assay of anxiety-related behavior in rodents. Nat Protoc 2:322–328. https://doi.org/10.1038/nprot.2007.44
25. Krolow R, Noschang CG, Arcego D et al (2010) Consumption of a palatable diet by chronically stressed rats prevents effects on anxiety-like behavior but increases oxidative stress in a sex-specific manner. Appetite 55:108–116. https://doi.org/10.1016/j.appet.2010.03.013
26. Dellu F, Fauchey V, Le Moal M, Simon H (1997) Extension of a new two-trial memory task in the rat: influence of environmental context on recognition processes. Neurobiol Learn Mem 67:112–120. https://doi.org/10.1006/nlme.1997.3746
27. Pandolfo P, Machado NJ, Köfalvi A et al (2013) Caffeine regulates frontocorticostriatal dopamine transporter density and improves attention and cognitive deficits in an animal model of attention deficit hyperactivity disorder. Eur Neuropsychopharmacol 23:317–328. https://doi.org/10.1016/j.euroneuro.2012.04.011
28. Netto CBO, Conte S, Leite MC et al (2006) Serum S100B protein is increased in fasting rats. Arch Med Res 37:683–686. https://doi.org/10.1016/j.arcmed.2005.11.005
29. Gottfried C, Tramontina F, Gonçalves D et al (2002) Glutamate uptake in cultured astrocytes depends on age: a study about the effect of guanosine and the sensitivity to oxidative stress induced by H(2)O(2). Mech Ageing Dev 123:1333–1340. https://doi.org/10.1016/s0047-6374(02)00069-6
30. Thomazi AP, Godinho GFRS, Rodrigues JM et al (2004) Ontogenetic profile of glutamate uptake in brain structures slices from rats: sensitivity to guanosine. Mech Ageing Dev 125:475–481. https://doi.org/10.1016/j.mad.2004.04.005
31. Wajner M, Sitta A, Kayser A et al (2019) Screening for organic acidurias and aminoacidopathies in high-risk Brazilian patients: eleven-year experience of a reference center. Genet Mol Biol 42:178–185. https://doi.org/10.1590/1678-4685-GMB-2018-0105
32. Minet R, Villie F, Marcollet M et al (1997) Measurement of glutamine synthetase activity in rat muscle by a colorimetric assay. Clin Chim Acta 268:121–132. https://doi.org/10.1016/s0009-8981(97)00173-3
33. Browne RW, Armstrong D (1998) Reduced glutathione and glutathione disulfide. Methods Mol Biol 108:347–352. https://doi.org/10.1385/0-89603-472-0:347
34. Leite MC, Galland F, Brolese G et al (2008) A simple, sensitive and widely applicable ELISA for S100B: methodological features of the measurement of this glial protein. J Neurosci Methods 169:93–99. https://doi.org/10.1016/j.jneumeth.2007.11.021
35. Tramontina F, Leite MC, Cereser K et al (2007) Immunoassay for glial fibrillary acidic protein: antigen recognition is affected by its phosphorylation state. J Neurosci Methods 162:282–286. https://doi.org/10.1016/j.jneumeth.2007.01.001
36. Bobermin LD, Roppa RHA, Quincozes-Santos A (2019) Adenosine receptors as a new target for resveratrol-mediated gliioprotection. Biochim Biophys Acta Mol basis Dis 1865:634–647. https://doi.org/10.1016/j.bbadis.2019.01.004
37. Livak KJ, Schmittgen TD (2001) Analysis of relative gene expression data using real-time quantitative PCR and the 2(-Delta Delta C(T)) method. Methods 25:402–408. https://doi.org/10.1006/meth.2001.1262
38. Peterson GL (1977) A simplification of the protein assay method of Lowry et al. which is more generally applicable. Anal Biochem 83:346–356. https://doi.org/10.1016/0003-2697(77)90043-4
39. Yang Y, Song W (2013) Molecular links between Alzheimer's disease and diabetes mellitus. Neuroscience 250:140–150. https://doi.org/10.1016/j.neuroscience.2013.07.009
40. Schalkwijk CG, Stehouwer CDA (2020) Methylglyoxal, a highly reactive dicarbonyl compound, in diabetes, its vascular complications, and other age-related diseases. Physiol Rev 100:407–461. https://doi.org/10.1152/physrev.00001.2019
41. Biessels GJ, Staekenborg S, Brunner E et al (2006) Risk of dementia in diabetes mellitus: a systematic review. Lancet Neurol 5:64–74. https://doi.org/10.1016/S1474-4422(05)70284-2
42. Kopf D, Frölich L (2009) Risk of incident Alzheimer's disease in diabetic patients: a systematic review of prospective trials. J Alzheimers Dis 16:677–685. https://doi.org/10.3233/JAD-2009-1011
43. Liu Y-W, Zhu X, Yang Q-Q et al (2013) Suppression of methylglyoxal hyperactivity by mangiferin can prevent diabetes-associated cognitive decline in rats. Psychopharmacology 228:585–594. https://doi.org/10.1007/s00213-013-3061-5
44. Angeloni C, Zambonin L, Hrelia S (2014) Role of methylglyoxal in Alzheimer's disease. Biomed Res Int 2014:1–12. https://doi.org/10.1155/2014/238485
45. Di Loreto S, Caracciolo V, Colafarina S et al (2004) Methylglyoxal induces oxidative stress-dependent cell injury and up-regulation of interleukin-1beta and nerve growth factor in cultured hippocampal neuronal cells. Brain Res 1006:157–167. https://doi.org/10.1016/j.brainres.2004.01.066
46. Di Loreto S, Zimmitti V, Sebastiani P et al (2008) Methylglyoxal causes strong weakening of detoxifying capacity and apoptotic cell death in rat hippocampal neurons. Int J Biochem Cell Biol 40:245–257. https://doi.org/10.1016/j.biocel.2007.07.019
47. Rabbani N, Thornalley PJ (2008) Dicarbonyls linked to damage in the powerhouse: glycation of mitochondrial proteins and oxidative stress. Biochem Soc Trans 36:1045–1050. https://doi.org/10.1042/BST0361045
48. Sena CM, Matafome P, Crisóstomo J et al (2012) Methylglyoxal promotes oxidative stress and endothelial dysfunction. Pharmacol Res 65:497–506. https://doi.org/10.1016/j.phrs.2012.03.004
49. Bélanger M, Yang J, Petit J-M et al (2011) Role of the glyoxalase system in astrocyte-mediated neuroprotection. J Neurosci 31:18338–18352. https://doi.org/10.1523/JNEUROSCI.1249-11.2011
50. Rabbani N, Xue M, Thornalley PJ (2014) Activity, regulation, copy number and function in the glyoxalase system. Biochem Soc Trans 42:419–424. https://doi.org/10.1042/BST20140008
51. Hovatta I, Tennant RS, Helton R et al (2005) Glyoxalase 1 and glutathione reductase 1 regulate anxiety in mice. Nature 438:662–666. https://doi.org/10.1038/nature04250
52. McMurray KMJ, Du X, Brownlee M, Palmer AA (2016) Neuronal overexpression of Glo1 or amygdalar microinjection of methylglyoxal is sufficient to regulate anxiety-like behavior in mice. Behav Brain Res 301:119–123. https://doi.org/10.1016/j.bbr.2015.12.026
53. Beeri MS, Moshier E, Schmeidler J et al (2011) Serum concentration of an inflammatory glycotoxin, methylglyoxal, is associated with increased cognitive decline in elderly individuals. Mech Ageing Dev 132:583–587. https://doi.org/10.1016/j.mad.2011.10.007
54. Huang X, Wang F, Chen W et al (2012) Possible link between the cognitive dysfunction associated with diabetes mellitus and the neurotoxicity of methylglyoxal. Brain Res 1469:82–91. https://doi.org/10.1016/j.brainres.2012.06.011

55. Srikanth V, Westcott B, Forbes J et al (2013) Methylglyoxal, cognitive function and cerebral atrophy in older people. J Gerontol A Biol Sci Med Sci 68:68–73. https://doi.org/10.1093/gerona/gls100
56. Thornalley PJ, Rabbani N (2011) Glyoxalase in tumourigenesis and multidrug resistance. Semin Cell Dev Biol 22:318–325. https://doi.org/10.1016/j.semcdb.2011.02.006
57. Coleman E, Judd R, Hoe L et al (2004) Effects of diabetes mellitus on astrocyte GFAP and glutamate transporters in the CNS. Glia 48:166–178. https://doi.org/10.1002/glia.20068
58. Coulter DA, Eid T (2012) Astrocytic regulation of glutamate homeostasis in epilepsy. Glia 60:1215–1226. https://doi.org/10.1002/glia.22341
59. Rose CF, Verkhratsky A, Parpura V (2013) Astrocyte glutamine synthetase: pivotal in health and disease. Biochem Soc Trans 41:1518–1524. https://doi.org/10.1042/BST20130237
60. Dringen R (2000) Metabolism and functions of glutathione in brain. Prog Neurobiol 62:649–671. https://doi.org/10.1016/s0301-0082(99)00060-x
61. Sedlak TW, Paul BD, Parker GM et al (2019) The glutathione cycle shapes synaptic glutamate activity. Proc Natl Acad Sci USA 116:2701–2706. https://doi.org/10.1073/pnas.1817885116
62. Gonçalves C-A, Leite MC, Nardin P (2008) Biological and methodological features of the measurement of S100B, a putative marker of brain injury. Clin Biochem 41:755–763. https://doi.org/10.1016/j.clinbiochem.2008.04.003
63. Steiner J, Bernstein H-G, Bielau H et al (2007) Evidence for a wide extra-astrocytic distribution of S100B in human brain. BMC Neurosci 8:2. https://doi.org/10.1186/1471-2202-8-2
64. Guerra MC, Tortorelli LS, Galland F et al (2011) Lipopolysaccharide modulates astrocytic S100B secretion: a study in cerebrospinal fluid and astrocyte cultures from rats. J Neuroinflammation 8:128. https://doi.org/10.1186/1742-2094-8-128
65. Dos Santos JPA, Vizuete A, Hansen F et al (2018) Early and persistent O-GlcNAc protein modification in the streptozotocin model of Alzheimer's disease. J Alzheimers Dis 61:237–249. https://doi.org/10.3233/JAD-170211
66. Peskind ER, Griffin WS, Akama KT et al (2001) Cerebrospinal fluid S100B is elevated in the earlier stages of Alzheimer's disease. Neurochem Int 39:409–413. https://doi.org/10.1016/s0197-0186(01)00048-1
67. Zimmer DB, Chessher J, Wilson GL, Zimmer WE (1997) S100A1 and S100B expression and target proteins in type I diabetes. Endocrinology 138:5176–5183. https://doi.org/10.1210/endo.138.12.5579
68. de Souza DF, Leite MC, Quincozes-Santos A et al (2009) S100B secretion is stimulated by IL-1beta in glial cultures and hippocampal slices of rats: likely involvement of MAPK pathway. J Neuroimmunol 206:52–57. https://doi.org/10.1016/j.jneuroim.2008.10.012
69. de Souza DF, Wartchow K, Hansen F et al (2013) Interleukin-6-induced S100B secretion is inhibited by haloperidol and risperidone. Prog Neuro-Psychopharmacol Biol Psychiatry 43:14–22. https://doi.org/10.1016/j.pnpbp.2012.12.001
70. Bianchi ME (2007) DAMPs, PAMPs and alarmins: all we need to know about danger. J Leukoc Biol 81:1–5. https://doi.org/10.1189/jlb.0306164
71. Xu J, Wang H, Won SJ et al (2016) Microglial activation induced by the alarmin S100B is regulated by poly(ADP-ribose) polymerase-1. Glia 64:1869–1878. https://doi.org/10.1002/glia.23026
72. Chu JMT, Lee DKM, Wong DPK et al (2016) Methylglyoxal-induced neuroinflammatory response in in vitro astrocytic cultures and hippocampus of experimental animals. Metab Brain Dis 31:1055–1064. https://doi.org/10.1007/s11011-016-9849-3